2.A.1 *Nuclear Physics* **A110** (1968) 441—462; © *North-Holland Publishing Co., Amsterdam*

ELASTIC SCATTERING OF SEVERAL HYDROGEN AND HELIUM ISOTOPES FROM TRITIUM

M. IVANOVICH, P. G. YOUNG † and G. G. OHLSEN †
Research School of Physical Sciences,
Australian National University, Canberra

Received 11 December 1967

Abstract: The elastic scattering of protons, deuterons, ^{3}He and ^{4}He particles from tritium has been investigated for bombarding energies between approximately 3 and 11 MeV. Excitation functions were taken at several angles in each case, and angular distributions of d-^{3}H, ^{3}He-^{3}H and ^{4}He-^{3}H scattering were obtained. In addition, cross-section data from ^{3}He-^{3}He and ^{4}He-^{3}He elastic scattering and from the ^{3}H(d, α)n reaction are reported. A broad anomaly was observed in the d-^{3}H elastic scattering measurements corresponding to an excitation energy of approximately 19 MeV in ^{5}He. Two resonances were observed in the ^{4}He-^{3}H measurements corresponding to excitation energies of 4.65 and 6.79 MeV in ^{7}Li. A phase shift analysis of the ^{4}He-^{3}H data was performed, and spin and parity assignments of $\frac{7}{2}^-$ and $\frac{5}{2}^-$ were obtained for the two resonances. No sharp structure was observed in the p-^{3}H or ^{3}He-^{3}H excitation functions.

E NUCLEAR REACTIONS ^{3}H(p, p), ^{3}H(d, d), ^{3}H(d, α), ^{3}H(^{3}He, ^{3}He), ^{3}He(^{3}He, ^{3}He), ^{3}H(α, α), ^{3}He(α, α), E = 3-11 MeV; measured $\sigma(E; \theta)$. ^{5}He deduced level, π. ^{7}Li deduced levels, J, π, l.

1. Introduction

The experiments described in this paper involve systems composed of from four to seven nucleons. The work was undertaken to acquire further knowledge of the energy level structure of some of the very light nuclei and to provide data which might be generally useful in extracting information on nuclear forces. The experiments involve primarily the elastic scattering of protons, deuterons, ^{3}He and ^{4}He particles from tritium corresponding to the compound nuclei ^{4}He, ^{5}He, ^{6}Li and ^{7}Li, respectively. More limited data on ^{3}He-^{3}He and ^{4}He-^{3}He elastic scattering and the ^{3}H (d, α)n reaction are also presented.

The material is divided into six sections. Sect. 2 deals with a description of the experimental equipment, the techniques employed and the probable errors in the measurements. Sects. 3-6 deal primarily with p-^{3}H, d-^{3}H, ^{3}He-^{3}H and ^{4}He-^{3}H elastic scattering, respectively. Each section gives a brief account of the state of knowledge about the compound nucleus involved, a description of the data obtained and a short discussion. The data are presented graphically and in tabular form.

† Now at the Los Alamos Scientific Laboratory, Los Alamos, New Mexico, USA.

2. Experimental apparatus and method

Beams of protons, deuterons, doubly charged ^{3}He and ^{4}He particles were provided by the ANU tandem accelerator. Beam currents of 0.05 to 1.00 μA were used. The beams were energy analysed by a 90° magnet whose calibration is known to 0.1 %. The maximum instability in beam energy is estimated to have been 5 keV. After energy analysis, the beams were deflected by a 30° magnet, passed through a pair of "tracking slits", a magnetic quadrupole lens and finally through two tantalum collimators with 1.5 mm aperture diam spaced 20 cm apart. A tantalum anti-scattering baffle with a 2.2 mm aperture was placed 10 cm behind each collimator disc.

Tritium gas was contained in a target assembly almost identical in design to that described by Ohlsen and Young [1]). The beam entered the 7.5 cm diam target through a 0.25 μm nickel foil. The beam passed out of the gas target through a 0.6 μm nickel foil and was collected by a Faraday cup whose acceptance half-angle was about 4°. The Faraday cup was equipped with magnetic and electrostatic suppression. The scattered and recoil particles passed out of the target assembly through a 6.25 μm aluminised mylar foil which was attached to the stainless steel frame by an ordinary epoxy resin. The scattered particles were collimated by a rectangular slit system consisting of nominally identical slits together with an anti-scattering baffle placed midway between the slits. The slit dimensions were 3×5 mm and the anti-scattering slit had an aperture of 5×7.5 mm.

Two independently rotatable surface-barrier detector systems were used simultaneously throughout the measurements. Pulses from the detectors were amplified with double-delay-line amplifier systems and were routed into separate 200-channel blocks of a 400-channel analyser. The routing pulses were obtained from single-channel analysers with windows set around the region of interest in each spectrum. The dead-time correction to the analyser ranged from about 2 % to 6 %.

The gas target was filled with tritium at a pressure of 25 mg Hg from a uranium tritide furnace [2]). Pressure in the target cell was measured to an absolute accuracy of about ± 0.1 mm by means of an aneroid manometer † which was periodically calibrated with an oil manometer. Hydrogen exchange presented the greatest problem in determining the net pressure of tritium in the target. The partial pressure of the hydrogen impurity was determined by comparing the intensity of the recoil proton group from the impurity with calibration measurements made with a known pressure of hydrogen in the gas target. A maximum error of 3 % in the measured cross sections resulted from uncertainties in the net tritium pressure.

A discussion of other possible sources of error with the present apparatus is given by Ohlsen and Young [1]). Taking into account all experimental uncertainties, a maximum systematic error of approximately 5 % is expected in the present measurements. In certain of the experiments other sources of error (in addition to statistical)

† Wallace and Tiernan, Inc., Belleville, New Jersey, USA.

were present which will be discussed in the relevant sections. The uncertainty in the lab detector angle is 0.1° in all cases.

Uncertainty in the thickness of the nickel entrance foil (20 %) and in the calibration of the 90° magnet (0.1 %) results in estimated errors in the bombarding energy of ±10 keV for the experiments with hydrogen beams and ±20 keV for the experiments with helium beams. The energy resolution at the centre of the gas target is estimated to be 10 keV for the measurements made with hydrogen beams and 25 keV for helium beams.

3. Proton-triton elastic scattering

A great deal of interest in the four-nucleon system has resulted from the discovery of the 20.1 keV excited state in ^{4}He. The experimental evidence for this state is quite strong and includes observations through p-^{3}H elastic scattering [3]) as well as through a number of reactions [4]). There is also evidence for several negative-parity states at

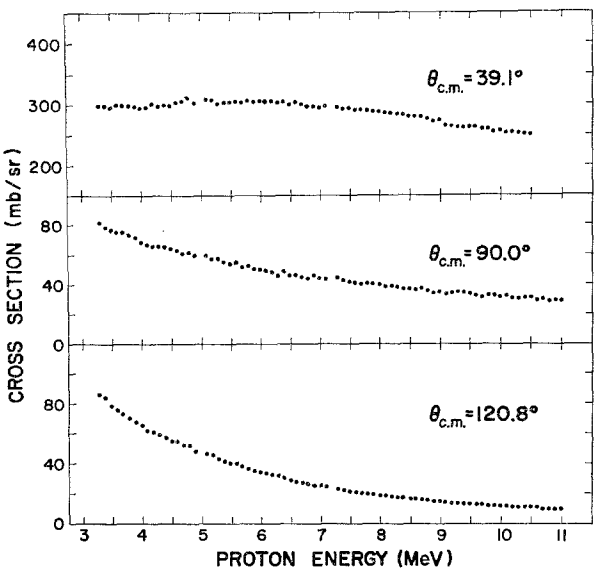

Fig. 1. Excitation functions for p-^{3}H elastic scattering. The differential cross section is given in the centre-of-mass system, and the energy scale is in the lab system.

slightly higher excitation energies in ^{4}He. For instance, theoretical studies by Barrett *et al.* [5]) suggest the presence of $T = 0$ states near 22 MeV (0^-) and 28 MeV (1^-) excitation energy, and Vlasov and Samoilov [6]) predict levels at 22 MeV (2^-) and 24 MeV (1^-). In addition, a phase-shift analysis of ^{3}He+p and ^{3}He+n scattering and polarization data suggests the presence of four negative-parity levels in ^{4}Li which should lie in the range 24-30 MeV excitation [7]) in ^{4}He.

In the present experiment, p-^{3}H elastic scattering cross sections were measured as a function of energy at $\theta_{c.m.} = 39.1°$, 90.0° and 120.8°. Data were taken in 100 keV steps for proton bombarding energies between 3.3 and 10.9 MeV corresponding to 22.3 to 28.0 MeV excitation in ^{4}He. The data are presented graphically in fig. 1 and numerically in table 1. The results given at $\theta_{c.m.} = 39.1°$ and 90.0° were obtained from the scattered proton group. The recoil tritons were observed for the data at 120.8°. The statistical error is 2 % or less for all the data. A comparison of these data with two angular distributions obtained by Brolley *et al.* [8]) reveals that five out of the six points which can be compared agree to within 3 %.

TABLE 1

p-^{3}He elastic scattering excitation function data

E_p (MeV)	σ(39.1°) (mb/sr)	σ(90.0°) (mb/sr)	σ(120.8°) (mb/sr)	E_p (MeV)	σ(39.1°) (mb/sr)	σ(90.0°) (mb/sr)	σ(120.8°) (mb/sr)
3.28	299	81.3	86.1	7.29	298	44.1	23.5
3.48	296	76.2	78.6	7.49	290	41.2	22.1
3.68	299	74.7	73.0	7.69	288	39.7	21.0
3.88	297	71.1	67.3	7.89	286	40.0	20.0
4.08	297	66.4	62.2	8.09	283	38.5	19.3
4.28	298	65.1	59.2	8.29	280	37.9	18.1
4.49	299	63.9	55.0	8.49	277	36.5	17.5
4.69	306	60.1	52.6	8.69	276	36.9	17.1
4.89	302	58.9	48.8	8.89	269	34.8	16.2
5.09	308	58.4	46.9	9.09	261	33.9	15.0
5.29	302	56.4	43.2	9.29	259	34.6	14.6
5.49	304	53.5	40.9	9.49	259	33.6	14.2
5.69	303	51.1	38.3	9.69	256	31.6	14.2
5.89	304	49.7	35.6	9.89	251	32.1	13.2
6.09	304	48.8	33.9	10.09	249	31.9	13.0
6.29	301	45.6	32.4	10.29	249	30.8	12.4
6.49	299	45.2	29.6	10.49	245	30.9	12.1
6.69	298	44.3	27.5	10.69		29.9	11.5
6.89	295	45.5	25.6	10.89		29.3	11.2
7.09	295	43.2	24.7				

The proton energy is given in the lab system. The scattering angle and cross section are in the centre-of-mass system.

As is seen in fig. 1, the cross section varies smoothly with energy and displays no sharp structure readily attributable to states in ^{4}He. Since states in this energy region would be expected to be quite broad, this result is not too surprising. It appears likely that more meaningful information on ^{4}He states at these energies could be obtained by means of a theoretical analysis incorporating ^{3}H(p, p)^{3}H, ^{3}He(n, n)^{3}He and ^{3}H (p, n)^{3}He cross section and polarization data.

4. Deuteron-triton elastic scattering

The energy levels in ^{5}He which are firmly established are the $\frac{3}{2}^-$ ground state, the $\frac{1}{2}^-$ first excited state at $\approx$ 2.6 MeV and the well-known [9]) $\frac{3}{2}^+$ state at 16.70 MeV. In addition, the presence of a broad state at about 20 MeV has been suspected for some time [10]), and recent measurements appear to confirm the existence of at least one state in this energy region. In particular, the d-^{3}H elastic scattering measurements of Tombrello *et al.* [11]) show a broad anomaly near 20 MeV excitation in ^{5}He. When these data are considered together with results from the ^{3}H(d, n)^{4}He reaction, a J^π assignment of $\frac{3}{2}^+$ or $\frac{5}{2}^+$ is indicated with the $\frac{5}{2}^+$ assignment requiring a mixed ^{4}D, ^{2}D configuration and the $\frac{3}{2}^+$ assignment requiring a ^{2}D state. However, in a study of the ^{7}Li(p, ^{3}He)^{5}He and ^{7}Li(p, t)^{5}Li reactions, Cerny *et al.* [12]) observed a peak at 19.9 MeV excitation in the former reaction but failed to see an effect in the latter reaction, indicating that a quartet state is involved with little doublet mixing. This result does not agree with either of the assignments suggested by Tombrello *et al.* [11]) since both require a substantial doublet component. It would therefore appear that either more than one level occurs around 20 MeV or that a large non-resonant background is present which makes the tentative assignments of Tombrello *et al.* invalid.

In the present experiment the d-^{3}H elastic scattering cross section was measured as a function of energy for deuteron energies between 2.6 and 11 MeV at ten centre-of-mass angles between 30.0° and 14.39°. This energy range corresponds to 18.2 MeV to 23.2 MeV excitation in ^{5}He. Energy steps of 100 or 200 keV were generally used, although smaller increments (50 keV) were used near the ^{3}H+p+n and ^{3}He+2n thresholds. In addition, an angular distribution was obtained at E_d = 7.00 MeV, and three excitation functions of the ^{3}H(d, α)n reaction were measured at fixed lab angles of 18.0°, 27.3° and 37.0°.

At most energies and angles used, the recoil triton group was not resolved from the impurity proton group. In order to utilize the triton information, the following procedure was used. The partial pressure of the hydrogen impurity was determined as described in sect. 2 by operating one of the detection systems at an angle where the proton group was resolved. The number of impurity counts in the unresolved triton-hydrogen peak of the other detection system was then obtained from measurements of the proton yield from d-p scattering with a known pressure of pure hydrogen in the target.

The elastic scattering excitation functions are presented graphically in fig. 2 and numerically in table 2. The data are given at 200 keV intervals. The results at angles of 106° and larger were obtained from the recoil triton group. Also included in fig. 2 are smooth curves drawn through a portion of the data of Stratton *et al.* [13]). At some angles it was necessary to interpolate the latter results. The statistical error in the present measurements is 2 % or less. The maximum systematic error is thought to be about 5 % (as discussed in sect. 2) except in the following cases. For energies below 5 MeV at $\theta_{c.m.}$ = 106° and 113° and for energies between 6 and 8 MeV at $\theta_{c.m.}$ =

143.9°, and additional error of up to 8 % is possible. This increased error results from uncertainty in the hydrogen impurity pressure and the fact that the impurity group was not resolved from the triton group in most cases.

The d-^{3}H angular distribution obtained at $E_d = 6.98$ MeV is given in fig. 3 and in table 3. The statistical error in the measurements is less than 1 %, and the additional error associated with the triton measurements is estimated to reach a maximum of about 5 % at the largest angle used.

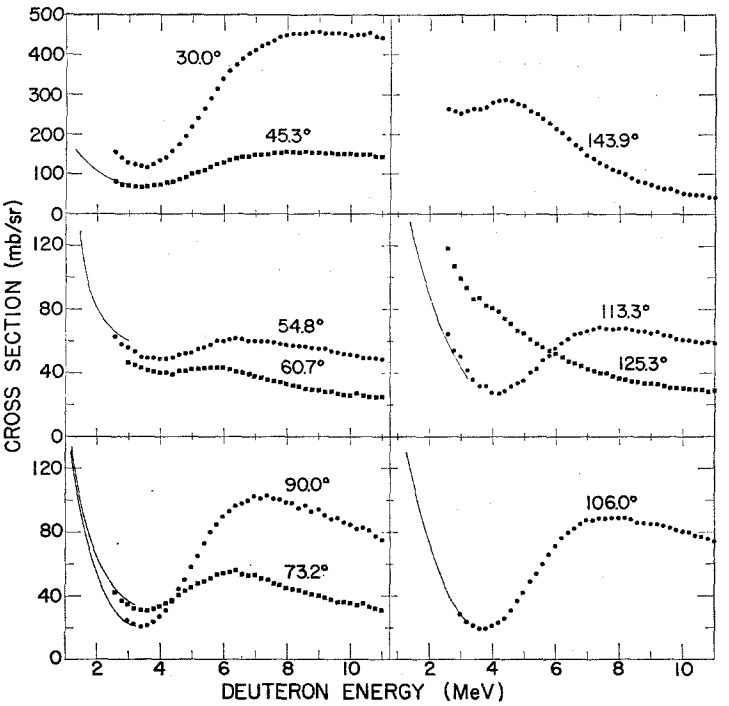

Fig. 2. Excitation functions for d-^{3}H elastic scattering. The differential cross section is given in the centre-of-mass system, and the energy scale is in the lab system. The solid curves represent the results of Stratton *et al.* [13]).

In most of the excitation functions, a broad interference dip is observed in the cross section at a deuteron energy of approximately 4 MeV. This energy corresponds to an excitation energy of 19.0 MeV in ^{5}He. At the largest angle used a broad peak occurs at this energy, whereas at $\theta_{c.m.} = 125.3°$ no significant effect is seen. The pronounced interference dip observed at $\theta_{c.m.} = 90°$ indicates that a positive-parity state is involved. Assuming a radius of 6 fm, the Wigner limit for an $l = 4$ state at this energy is 155 keV. Since the observed anomaly appears to be greater than 1 MeV in width, the present data suggest an orbital angular momentum of $l = 0$ or 2 is involved in the resonance, assuming that only one level is present.

TABLE 2
d-^{3}H elastic scattering excitation function data

E_d (MeV)	σ(30.0°) (mb/sr)	σ(45.3°) (mb/sr)	σ(54.8°) (mb/sr)	σ(60.7°) (mb/sr)	σ(73.2°) (mb/sr)	σ(90.0°) (mb/sr)	σ(106.0°) (mb/sr)	σ(113.3°) (mb/sr)	σ(125.3°) (mb/sr)	σ(143.9°) (mb/sr)
2.57	157	81.8	62.9		41.8			63.8	117.8	261.8
2.77	141	74.1	58.1		37.0			53.9	106.7	256.1
2.97	129	70.7	55.8	46.4	34.6	24.6	28.4	50.5	98.7	252.4
3.17	125	68.3	53.5	45.0	31.9	22.6	24.1	42.1	93.5	257.8
3.37	119	66.3	49.7	42.7	30.9	21.3	21.6	35.8	86.2	264.8
3.57	116	68.6	49.1	41.4	30.6	21.5	19.6	32.1	87.2	264.4
3.77	122	70.1	49.5	40.6	32.3	23.8	19.6	31.7	81.7	268.8
3.97	132	74.2	48.5	39.8	33.2	26.9	21.2	27.6	80.6	280.9
4.18	140	76.2	49.1	40.2	34.9	30.7	23.2	27.3	78.5	284.3
4.38	157	80.7	49.8	39.3	37.2	36.8	26.1	28.7	74.3	285.9
4.58	177	86.4	51.5	40.6	40.6	43.7	31.2	31.8	71.3	284.4
4.78	195	92.5	52.2	41.3	42.9	49.9	36.8	33.8	66.4	276.4
4.98	218	99.7	53.4	42.1	45.3	58.3	41.9	35.6	65.0	272.0
5.18	239	105.3	55.1	42.1	47.8	65.2	48.8	40.4	61.3	258.4
5.38	264	110.2	56.4	42.7	49.3	73.1	54.2	43.3	58.3	251.1
5.58	291	118.0	57.9	42.9	51.0	80.0	60.0	48.1	55.9	239.7
5.78	315	124.1	59.8	43.1	53.1	84.6	66.0	50.8	53.8	227.4
5.98	338	127.6	60.2	42.7	54.0	89.8	71.5	55.6	51.9	214.9
6.18	359	134.9	60.7	41.6	54.7	93.1	76.4	58.7	50.0	203.7
6.38	375	138.4	61.4	40.8	56.1	96.6	79.8	61.4	47.2	189.4
6.58	390	142.8	61.1	39.9	53.8	98.0	82.6	64.0	46.0	173.2
6.78	402	144.7	60.3	39.0	52.6	100.0	85.4	64.7	44.5	163.0
6.98	413	146.9	59.7	38.3	53.2	102.4	88.3	66.0	42.4	147.4
7.18	422	148.6	59.4	36.8	51.1	101.3	87.9	67.4	41.5	138.2
7.38	429	150.2	59.5	35.8	50.0	102.7	88.7	68.7	40.1	128.7
7.58	437	151.9	58.8	34.8	48.1	101.2	89.1	67.9	39.7	121.4
7.78	443	152.6	58.0	34.1	46.9	100.6	88.9	68.6	37.7	112.1
7.98	447	153.5	57.6	33.0	45.2	98.7	88.7	67.9	36.6	105.9
8.18	450	153.7	56.8	31.9	44.3	98.1	88.9	67.7	36.1	99.2
8.38	452	153.3	56.7	31.5	43.6	95.3	88.6	66.9	34.8	90.4
8.58	453	154.5	56.4	29.9	41.8	96.8	86.6	66.5	35.0	83.5
8.78	457	152.7	55.4	29.4	41.1	93.3	85.7	66.5	33.6	78.7
8.99	456	152.9	54.9	28.9	39.9	93.7	85.6	64.7	33.5	74.4
9.19	453	149.6	54.9	28.3	39.0	90.4	85.0	66.2	33.0	68.0
9.39	452	151.0	53.5	28.4	37.8	88.1	83.7	63.4	31.9	63.9
9.59	453	150.3	53.0	27.2	36.1	88.8	82.7	63.1	31.0	64.6
9.79	452	150.1	52.0	26.5	35.9	85.8	81.6	61.6	30.5	56.4
9.99	449	149.6	51.6	26.2	35.4	84.4	80.4	61.2	30.5	51.8
10.19	450	148.0	50.6	26.9	33.9	81.9	80.1	60.7	29.8	50.0
10.39	449	148.8	49.6	25.6	34.9	83.1	78.3	59.4	29.4	48.8
10.59	455	146.5	49.3	25.3	32.7	81.0	77.4	59.0	29.6	47.3
10.79	445	143.5	49.4	24.9	32.2	77.4	76.1	59.7	28.5	42.5
10.99	443	142.4	49.1	25.0	31.1	75.1	74.3	58.7	28.8	39.9

The deuteron energy is given in the lab system. The scattering angle and cross section are in the centre-of-mass system.

A comparison of the present results with the angular distribution data of Brolley *et al.* [8]) obtained at 5.6, 5.9 and 8.3 MeV (4 % quoted error) shows an rms average

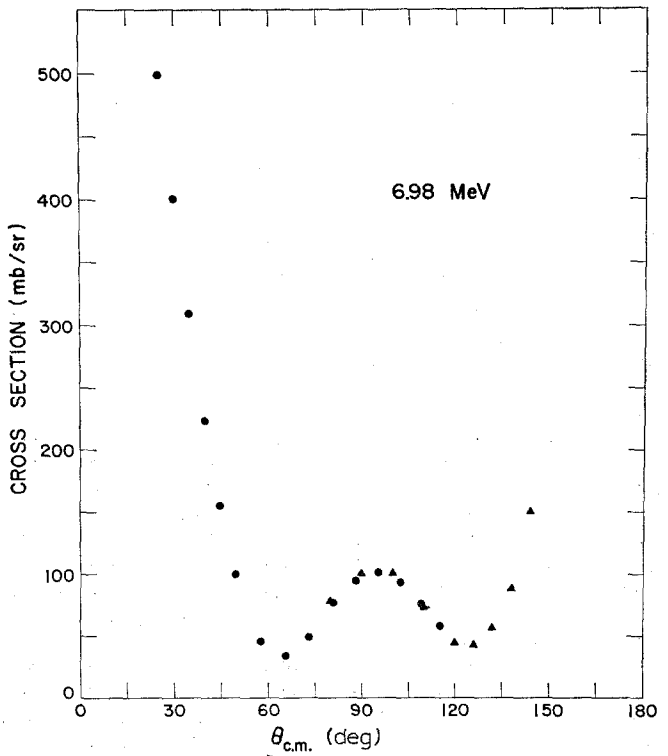

Fig. 3. Angular distribution of d-^{3}H elastic scattering for a deuteron lab energy of 6.98 MeV. The differential cross section is given in the centre-of-mass system. The triangles indicate data obtained via the recoil triton group.

TABLE 3

d-^{3}H elastic scattering angular distribution data at a deuteron energy of 6.98 MeV

$\theta_{c.m.}$ (degrees)	$\sigma(\theta)$ (mb/sr)	$\theta_{c.m.}$ (degrees)	$\sigma(\theta)$ (mb/sr)
25.0	499.2	90.0	101.4*
29.9	401.5	95.3	102.0
34.8	309.4	100.0	101.1*
39.8	223.6	102.2	94.2
44.7	156.0	108.9	76.8
49.5	100.6	110.0	73.5*
57.5	46.5	115.2	58.7
65.4	34.7	120.0	45.2*
73.2	49.7	126.0	43.5*
80.0	78.8*	132.0	57.2*
80.8	75.5	138.0	98.0*
88.2	94.8	144.0	151.0*

The cross section is given in the centre-of-mass system. The asterisks indicate data obtained from the recoil triton group.

percent deviation of about 5 %. The present measurements also agree within quoted errors with three of the four excitation functions obtained by Tombrello *et al.* [11]); however, the data given by Tombrello *et al.* for $\theta_{c.m.} = 54.8°$ are systematically 15-20 % higher than the present results.

No significant anomaly was observed in the excitation functions in the vicinity of the $^3H+n+p$ and $^3He+2n$ thresholds. If such an effect does occur, our results indicate that it is of the order of a few percent at most.

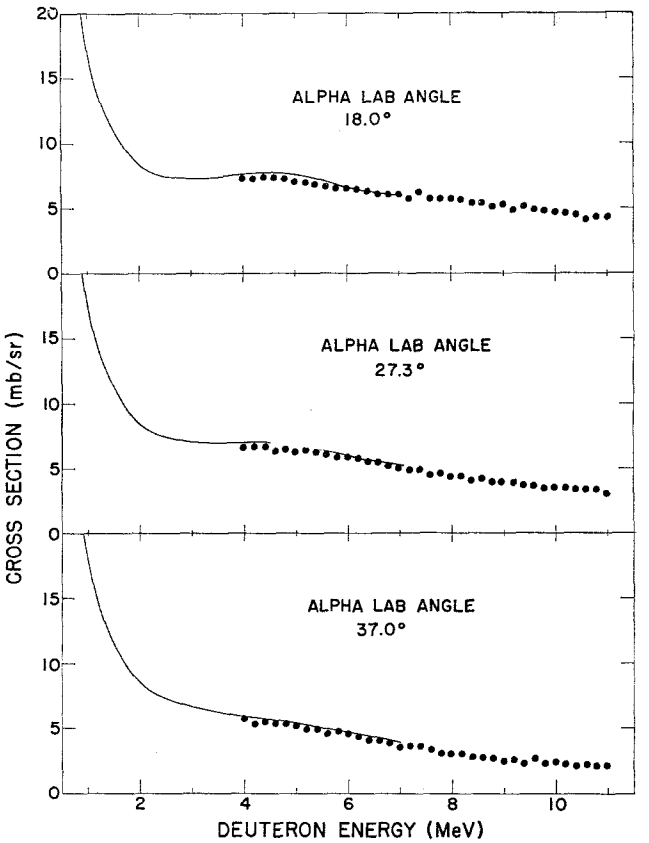

Fig. 4. Excitation functions for the $^3H(d, \alpha)n$ reaction. The differential cross section is given in the centre-of-mass system, and the energy scale is in the lab system. The solid curves represent the results of Bame and Perry [10]).

The $^3H(d, \alpha)n$ excitation functions are included in fig. 4 and table 4. The statistical error in these measurements is 3 % or less. The smooth curves given in the figure describe the $^3H(d, n)^4He$ measurements of Bame and Perry [10]). These authors fit Legendre expansions to their results, and the curves of fig. 4 were computed from the listed coefficients. Unfortunately, the present $^3H(d, \alpha)n$ measurements do not completely span the region of the resonance seen in the d-^3H scattering measurements.

It is therefore, not possible to confirm the presence of the broad shoulder seen in the data of Bame and Perry at $\theta_{lab} = 18.0°$.

TABLE 4

Excitation functions for the ^{3}H(d, α)n reaction

θ_{lab}	18.0°	27.3°	37.0°	θ_{lab}	18.0°	27.3°	37.0°
E_d (MeV)	$\sigma(\theta)$ (mb/sr)	$\sigma(\theta)$ (mb/sr)	$\sigma(\theta)$ (mb/sr)	E_d (MeV)	$\sigma(\theta)$ (mb/sr)	$\sigma(\theta)$ (mb/sr)	$\sigma(\theta)$ (mb/sr)
3.97	7.29	6.61	5.70	7.58	5.67	4.52	3.29
4.18	7.24	6.68	5.36	7.78	5.79	4.65	3.07
4.38	7.39	6.64	5.51	7.98	5.70	4.38	3.01
4.58	7.30	6.36	5.39	8.18	5.64	4.43	3.04
4.78	7.25	6.51	5.34	8.39	5.40	4.10	2.82
4.98	7.01	6.31	5.18	8.58	5.38	4.20	2.76
5.18	6.97	6.41	4.94	8.79	5.17	3.96	2.72
5.38	6.79	6.33	4.97	8.99	5.33	3.93	2.53
5.58	6.67	6.09	4.56	9.19	4.81	3.93	2.63
5.78	6.57	5.93	4.74	9.39	5.11	3.71	2.32
5.98	6.51	5.94	4.45	9.59	4.96	3.64	2.69
6.18	6.52	5.82	4.36	9.79	4.82	3.52	2.28
6.38	6.28	5.57	4.04	9.99	4.66	3.56	2.39
6.58	6.12	5.49	4.01	10.19	4.64	3.51	2.25
6.78	6.12	5.24	3.81	10.39	4.54	3.40	2.16
6.98	6.07	5.01	3.56	10.59	4.16	3.36	2.19
7.18	5.77	4.89	3.67	10.79	4.24	3.37	2.14
7.38	6.20	4.88	3.59	10.99	4.27	3.06	2.13

The deuteron energy is given in the lab system. The cross section is in the centre-of-mass system.

5. The ^{3}He-^{3}H elastic scattering

While some data are available on ^{3}He-^{3}He elastic scattering [9]), the experimental information on ^{3}He-^{3}H scattering is very limited. In particular, the only reported [14]) measurements are a set of ^{3}He-^{3}H (and ^{3}He-^{3}He) angular distributions taken at ^{3}He energies between 12 and 25 MeV. Thus it was considered of interest to investigate the excitation region between 18 and 22 MeV in ^{6}Li by means of ^{3}He-^{3}H elastic scattering.

The data consist of three excitation functions taken at centre-of-mass angles 40°, 90° and 140° for ^{3}He bombarding energies between 4.4 and 12 MeV corresponding to 18.0-21.8 MeV excitation in ^{6}Li. The latter two excitation curves were obtained from the recoil triton group. In addition, four angular distributions of ^{3}He-^{3}H scattering were obtained at ^{3}He bombarding energies of 5, 7, 9 and 11 MeV. For the purpose of comparison, ^{3}He-^{3}He angular distributions were also measured at 9 and 11 MeV.

The excitation function data are presented in fig. 5 and table 5. As is seen from the figure, the excitation functions are structureless, and the cross section decreases monotonically with energy at each of the three angles. The ^{3}He-^{3}H angular distri-

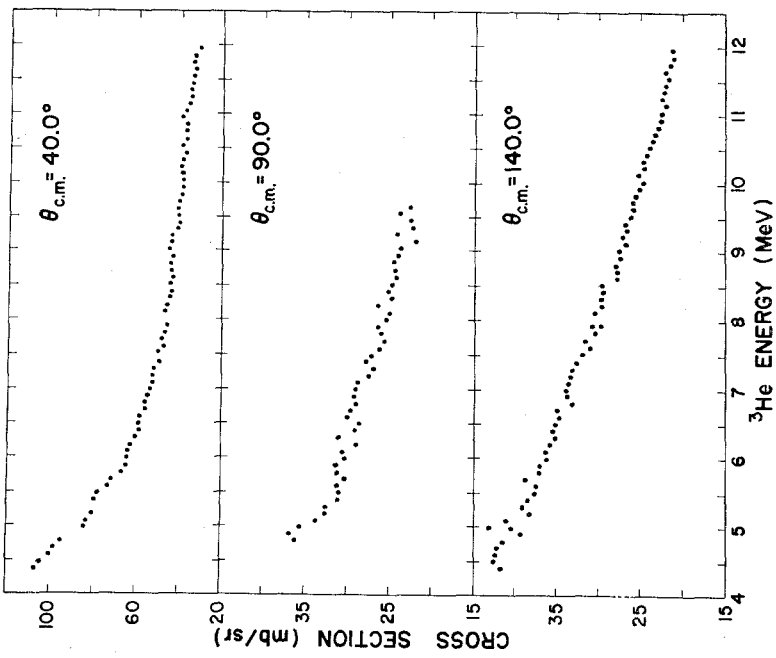

Fig. 5. Excitation functions for ^{3}He-^{3}H elastic scattering. The differential cross section is given in the centre-of-mass system and the energy scale in the lab system.

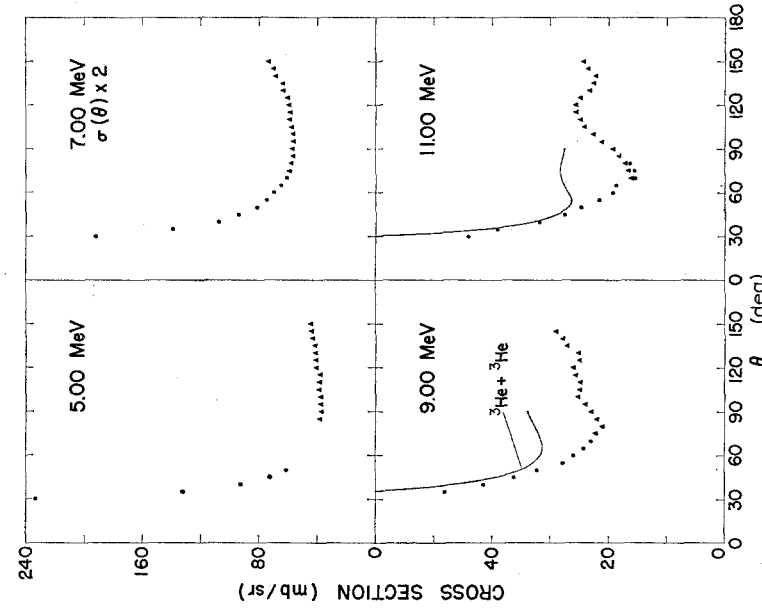

Fig. 6. Angular distributions of ^{3}He-^{3}H elastic scattering for ^{3}He lab energies of 5, 7, 9 and 11 MeV. The differential cross section is given in the centre-of-mass system. The solid curves are visual fits to the ^{3}He-^{3}He angular distributions of fig. 7. The triangles indicate data obtained via the recoil triton group.

butions are given in fig. 6. The triangles indicate data obtained via the recoil triton group. The curves given with the 9 and 11 MeV data are visual fits to the ^{3}He-^{3}He angular distributions given in fig. 7. The angular distributions are given in tabular form in table 6.

TABLE 5

^{3}He-^{3}H elastic scattering excitation functions

$E_{^3He}$ (MeV)	σ(40.0°) (mb/sr)	σ(90.0°) (mb/sr)	σ(140.0°) (mb/sr)	$E_{^3He}$ (MeV)	σ(40.0°) (mb/sr)	σ(90.0°) (mb/sr)	σ(140.0°) (mb/sr)
4.48	104.6	41.5	42.5	8.12	46.6	24.9	30.3
4.68	98.3	40.9	42.0	8.32	44.5	24.6	29.5
4.89	89.5	36.7	39.2	8.52	44.0	24.6	29.5
5.09	83.2	33.6	40.9	8.72	43.8	24.2	27.8
5.29	79.7	32.6	39.0	8.92	42.9	23.8	27.2
5.50	75.4	30.9	37.5	9.13	43.8	21.8	26.7
5.70	71.0	30.2	38.6	9.33	40.9	22.1	26.5
5.90	64.2	31.3	35.9	9.53	40.1	23.7	26.0
6.10	63.7	30.5	36.3	9.73	39.8		25.9
6.30	60.0	30.9	35.0	9.93	38.4		24.9
6.51	58.7	28.5	35.0	10.13	38.7		25.2
6.71	55.8	29.5	34.7	10.33	38.4		24.6
6.91	54.6	29.1	33.7	10.53	38.2		23.9
7.11	52.8	28.7	33.6	10.73	36.7		23.1
7.31	51.7	26.7	32.9	10.93	38.4		22.5
7.51	49.7	27.0	31.8	11.13	35.2		21.9
7.72	47.7	25.5	31.6	11.33	33.9		22.2
7.92	45.6	26.3	30.1	11.54	32.9		21.7
				11.74	33.5		21.5
				11.94	30.0		21.2

The ^{3}He energy is given in the lab system. The scattering angle and cross section are in the centre-of-mass system.

The statistical error in the above results is approximately 2 %. Besides the systematic error discussed in sect. 2, an additional error of about 3 % results from uncertainty in a background correction made to the data. This correction was required for background protons and alpha particles from the ^{3}H(^{3}He, p)nα and ^{3}He(^{3}He, p)pα reactions.

The present ^{3}He-^{3}He and ^{3}He-^{3}H angular distributions are included in data fit by Thompson and Tang using the resonating-group method [15]). Evidence for a number of levels in ^{6}He and ^{6}Li was found in this study.

6. The ^{4}He-^{3}H elastic scattering

From a phase-shift analysis of ^{3}He-^{4}He elastic scattering cross sections, Tombrello and Parker [16]) established the presence of a $^2F_{\frac{5}{2}}$ level in ^{7}Be at an excitation

TABLE 6

^{3}He-^{3}H and ^{3}He-^{3}He elastic scattering angular distribution data

$E_{^3He}$ (MeV)	^{3}He-^{3}H				^{3}He-^{3}He		
	5.00	7.00	9.00	11.00	9.08	11.07	
$\theta_{c.m.}$ (degrees)	$\sigma(\theta)$ (mb/sr)	$\sigma(\theta)$ (mb/sr)	$\sigma(\theta)$ (mb/sr)	$\sigma(\theta)$ (mb/sr)	$\sigma(\theta)$ (mb/sr)	$\sigma(\theta)$ (mb/sr)	Particle detected
30.0	233.4	96.2		44.1	108.2	65.2	^{3}He
35.0	132.2	69.8	48.1	39.1	65.3	42.1	^{3}He
40.0	92.7	54.1	41.4	31.8	46.8	32.7	^{3}He
45.0	72.8	47.2	36.3	27.5	39.9	29.1	^{3}He
50.0	61.1	40.7	32.2	24.7	35.2	26.8	^{3}He
55.0		37.5	27.8	21.5	32.9	26.0	^{3}He
60.0		35.0	26.0	19.2	31.9	26.7	^{3}He
65.0		32.5	24.2	18.7	31.0	27.6	^{3}He
70.0		30.5	22.9	15.4	31.5	27.5	^{3}He
70.0				16.1			t
75.0		29.5	22.1	15.5	32.1	28.9	^{3}He
75.0		29.7	22.2	16.5			t
80.0			20.9	16.2	32.4	27.9	^{3}He
80.0		29.1	20.9	17.1			t
85.0					33.3	27.6	^{3}He
85.0	38.4	28.5	21.9	18.1			t
90.0					34.9	27.7	^{3}He
90.0	37.1	28.8	22.4	19.2			t
95.0	37.6	28.4	23.9	21.1			t
100.0	37.6	28.5	25.4	22.6			t
105.0	38.7	29.0	24.8	24.1			t
110.0	38.3	29.6	24.7	24.8			t
115.0	38.0	29.5	25.6	25.6			t
120.0	40.5	29.7	25.9	25.6			t
125.0	40.9	30.2	24.9	24.8			t
130.0	41.1	31.7	25.1	23.2			t
135.0	41.7	31.9	27.1	22.5			t
140.0	43.1	34.5	27.8	22.2			t
145.0	43.6	35.3	28.7	23.6			t
150.0	44.2	36.9		24.3			t

The ^{3}He energy is given in the lab system. The cross section is in the centre-of-mass system.

energy of 6.51 MeV and verified the existence of a $^2F_{\frac{7}{2}}$ level at 4.54 MeV. The purpose of the present work is to study the corresponding levels in the mirror nucleus ^{7}Li by means of ^{4}He-^{3}H elastic scattering. In the case of ^{7}Li, both these levels have been observed through other reactions, but the spin assignments are listed as tentative [9]).

The ^{4}He-^{3}H elastic scattering angular distributions were obtained at alpha bombarding energies of 5.07, 6.64, 8.20, 9.76 and 10.92 MeV. The data cover the angular range $\theta_{c.m.} = 31.6°$ to 153.0°. Excitation functions of ^{4}He-^{3}H scattering were obtained at six angles for alpha energies of approximately 4.2 MeV to 10.9 MeV.

This energy range corresponds to 4.3-7.2 MeV excitation in ^{7}Li. Also obtained were excitation functions of ^{4}He-^{3}He scattering at three angles for alpha energies between 5.9 MeV and 7.9 MeV corresponding to 4.1-5.0 MeV excitation in ^{7}Be. The ^{4}He-^{3}H and ^{4}He-^{3}He measurements were performed with the same gas target, entrance foil etc. in order to measure accurately the difference in energy of the $^{2}F_{\frac{7}{2}}$ level in ^{7}Li and ^{7}Be. Lab energy steps of 50 keV were used in the excitation functions where the cross section changes rapidly and 100 keV steps elsewhere.

A phase-shift analysis of the data was carried out using the formulae of Critchfield and Dodder for the elastic scattering of spin $\frac{1}{2}$ from spin 0 particles [17]). The phase

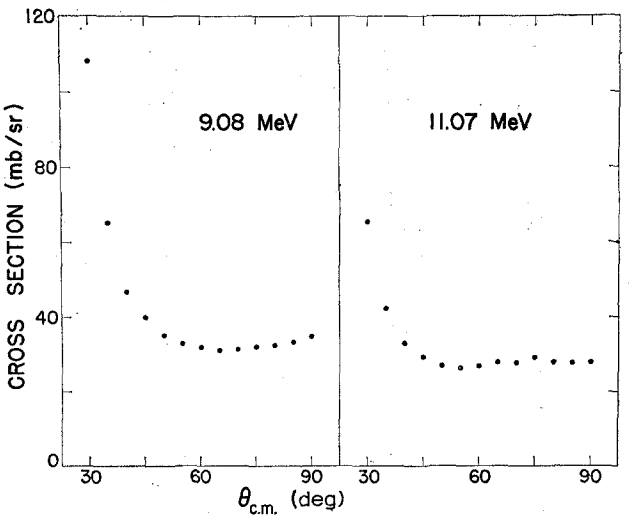

Fig. 7. Angular distributions of ^{3}He-^{3}He elastic scattering for ^{3}He lab energies of 9.08 and 11.07 MeV. The differential cross section is given in the centre-of-mass system.

shifts were extracted in the following manner. Using the ^{4}He-^{3}He phase shifts of Tombrello and Parker as initial values [16]), each phase shift was varied an amount proportional to the partial derivative of χ^2 with respect to that phase shift, where χ^2 is given by

$$\chi^2 = \sum_i \left[\frac{\sigma_{\exp}(\theta_i) - \sigma_{\text{calc}}(\theta_i)}{\sigma_{\exp}(\theta_i)}\right]^2.$$

The new value of χ^2 was compared with the old value, and the process was repeated until a minimum χ^2 was found. This procedure was then repeated several times using the newly-extracted phase shifts as a starting point and reducing the size of the phase shift variation increments. Phase shifts through $l = 3$ were allowed in the analysis. Only real phase shifts were used since ^{4}He + ^{3}H is the only particle channel open in the energy range studied.

The ^{4}He-^{3}H angular distributions are presented graphically in fig. 8 and numerically in table 7. The statistical error in the data is 2 % or less. The curves shown with the data represent the fits obtained with the phase shifts given in table 8. The phase shifts in the table are labelled δ_l^+ and δ_l^- for total angular momentum $j = l+\frac{1}{2}$ and $j = l-\frac{1}{2}$, respectively. The fits were obtained by allowing all the phase shifts to vary except δ_2^+ and δ_2^- which were held fixed at values computed from a charged hard

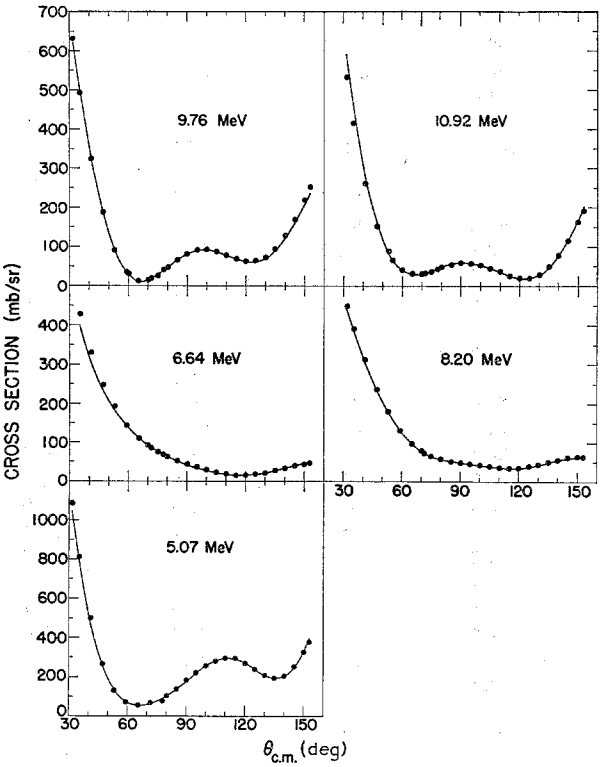

Fig. 8. Angular distributions of ^{4}He-^{3}H elastic scattering for ^{4}He lab energies of 5.07, 6.64, 8.20, 9.76 and 10.92 MeV. The differential cross section is given in the centre-of-mass system. The solid curves represent the fits obtained with the phase shifts of table 8.

sphere of radius 2.8 fm. These D-wave phase shifts are consistent with those extracted when all the phase shifts were allowed to vary (not presented).

The ^{4}He-^{3}H excitation functions are presented in fig. 9 and in table 9. The data are given in 200 keV intervals except near the $^2F_{\frac{7}{2}}$ resonance. The statistical error is 2 % or less except at the 5.1 MeV minimum in the 65.3° excitation curve where the error gets as large as 15 %. The prominent features of these data are two resonances located at alpha energies of approximately 5 MeV and 10 MeV. The similar behaviour of the cross section at the two resonances suggests that the same l-value is involved in both cases in agreement with results from ^{3}He-^{4}He scattering measurements [16]).

TABLE 7

^{3}He-^{4}H elastic scattering angular distribution data

E_α(MeV)	5.07	6.64	8.20	9.76	10.92	
$\theta_{c.m.}$ (deg)	$\sigma(\theta)$ (mb/sr)	$\sigma(\theta)$ (mb/sr)	$\sigma(\theta)$ (mb/sr)	$\sigma(\theta)$ (mb/sr)	$\sigma(\theta)$ (mb/sr)	Particle detected
31.6	1086.0		449.1	631.9	532.7	α
35.1	812.0	428.1	392.5	490.4	416.5	α
41.0	501.2	330.8	312.5	325.4	262.6	α
47.0	266.0	246.9	238.3	188.5	152.9	α
53.0	131.0	191.6	180.1	90.6	88.7	α
55.0					67.6	t
59.1	71.0	143.4	130.9	35.3	44.0	α
60.0				31.5	41.8	t
65.0			97.5	14.0	31.0	t
65.3	54.4	109.2	96.0	13.5	30.9	α
70.0		92.3	80.2	14.5	30.7	t
71.6	68.5	85.1	72.4	19.0	32.6	α
75.0		74.8	66.5	27.1	35.4	t
78.0	76.3	68.2		40.5	43.3	α
80.0	99.0	64.5	57.3	47.7	45.8	t
84.6				64.7		α
85.0	137.8	53.4	49.5	66.9	52.5	t
90.0	179.9	44.1	46.9	83.2	58.5	t
95.0	221.0	36.1	45.9	91.6	56.8	t
100.0	256.7	28.7	41.7	92.5	52.7	t
105.0	277.6	22.5	38.2	88.3	44.0	t
110.0	293.5	17.2	36.2	78.7	36.1	t
115.0	292.9	14.2	34.9	70.0	25.8	t
120.0	270.4	14.7	36.0	62.7	19.5	t
125.0	238.2	17.8	39.7	64.5	19.7	t
130.0	209.9	21.4	43.8	73.4	28.4	t
135.0	194.3	27.1	51.3	94.6	51.0	t
140.0	204.3	33.3	56.7	128.7	79.3	t
145.0	254.5	39.1	62.4	169.2	117.4	t
150.0	328.2	42.1	64.2	218.1	164.2	t
153.0	379.7	45.7	63.8	252.2	191.9	t

The alpha energy is given in the lab system. The cross section is in the centre-of-mass system.

TABLE 8

^{4}He-^{3}H elastic scattering phase shifts

E_α (MeV)	δ_0 (deg)	δ_1^+ (deg)	δ_1^- (deg)	δ_2^+ (deg)	δ_2^- (deg)	δ_3^+ (deg)	δ_3^- (deg)
5.07	−46.2	153.6	150.2	−1.1	−1.1	78.1	3.3
6.64	−57.1	146.7	144.9	−2.2	−2.2	173.4	5.1
8.20	−64.6	140.1	135.2	−3.6	−3.6	173.8	21.6
9.76	−56.3	138.4	133.5	−5.3	−5.3	171.8	76.3
10.92	−65.6	129.9	124.1	−6.8	−6.8	174.0	121.5

The fits obtained with these phase shifts are shown in fig. 8.

Since excitation data were obtained at only six angles, it was necessary to restrict some of the phase shifts in order to obtain meaningful fits to these data. Accordingly, the P-wave phase shifts were constrained to be unsplit and to have values calculated from a charged hard sphere of radius 3.8 fm. This choice of radius produces phase shifts which agree well with those extracted from the angular distributions (table 8). The D-wave phase shifts were likewise constrained to hard-sphere values for a radius

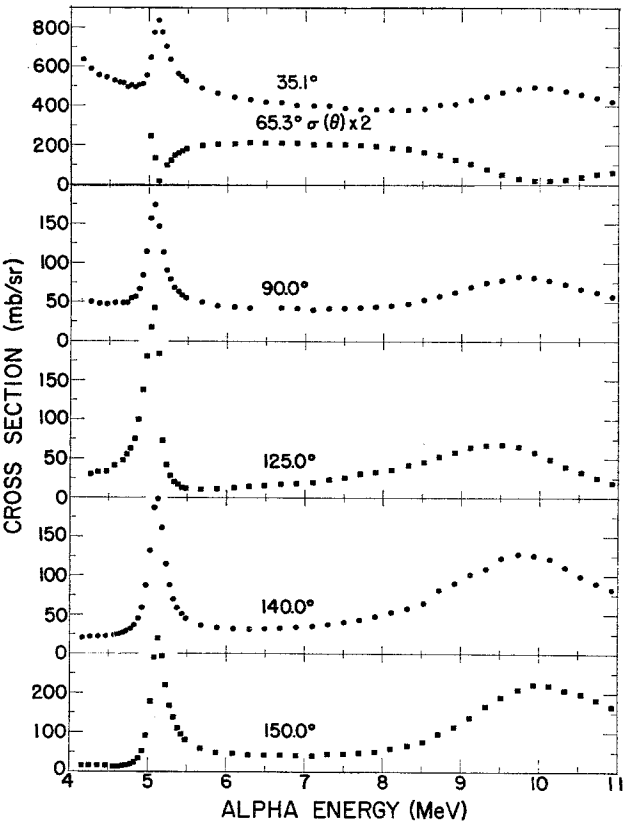

Fig. 9. Excitation functions of ^{4}He-^{3}H elastic scattering. The scattering angles and differential cross section are given in the centre-of-mass system. The energy scale is in the lab system.

$R = 3.0$ fm. With these constraints fits were obtained to the measured cross sections at each energy by allowing δ_0, δ_3^+ and δ_3^- to vary as described earlier.

The values of δ_0, δ_3^+ and δ_3^- extracted in this manner are given by the points in fig. 10. From the behaviour of δ_3^+ and δ_3^-, it is clear that the two resonances have $J^\pi = \frac{7}{2}^-$ and $\frac{5}{2}^-$. The solid curves labelled δ_1 and δ_2 are the hard-sphere values used in fitting the data. The solid curve associated with δ_0 represents hard-sphere values computed for $R = 2.8$ fm. This latter curve is included merely to illustrate the deviation of δ_0 from the hard-sphere values.

TABLE 9

^{4}He-^{3}H elastic scattering excitation function data

E_α (MeV)	σ(35.1°) (mb/sr)	σ(65.3°) (mb/sr)	σ(90.0°) (mb/sr)	σ(125.0°) (mb/sr)	σ(140.0°) (mb/sr)	σ(150.0°) (mb/sr)
4.16	637.9				21.5	16.3
4.26	590.4		49.9	29.9	21.7	15.4
4.36	565.2		48.7	33.1	21.9	15.4
4.46	547.5		47.3	34.2	23.1	13.9
4.56	533.4		49.1	41.1	24.6	13.4
4.62	521.0				25.5	13.4
4.67	519.8		49.1	48.4	27.5	13.6
4.72	500.5		49.0	55.2	29.2	15.2
4.767	504.7		54.7	63.1	33.0	18.2
4.818	502.4		57.9	75.5	37.6	23.2
4.869	508.2		67.0	100.4	45.8	31.6
4.920	515.1		85.0	136.7	59.4	51.4
4.970	558.5		115.0	179.9	86.9	91.4
5.021	653.2	123.7	157.8	217.7	133.0	177.2
5.072	778.2	68.2	175.2	243.1	186.3	290.3
5.123	843.4	9.2	147.5	184.0	197.9	339.4
5.173	783.3		113.8	71.8	161.0	294.0
5.225	703.9	49.0	90.6	41.1	114.7	218.6
5.275	642.7	63.1	79.7	27.2	87.7	165.6
5.325	602.5	76.6	69.4	20.1	69.6	137.6
5.376	568.3	81.3	64.4	14.4	58.7	110.6
5.427	548.6	85.6	58.7	13.0	51.0	94.5
5.477	528.7	89.6	55.6	11.5	45.2	81.4
5.68	487.7	99.5	49.8	10.0	35.9	59.2
5.88	463.6	103.0	45.5	11.3	33.2	49.0
6.09	443.7	104.1	44.3	12.8	31.0	45.8
6.29	432.9	106.4	42.4	13.8	31.3	41.8
6.49	421.1	106.0		15.5	32.6	42.1
6.69	416.8	107.4	41.7	16.7	32.2	40.9
6.89	404.6	105.5	41.4	18.3	33.8	40.4
7.10	403.3	102.9	40.0	19.4	34.5	40.1
7.30	396.6	102.8	41.2	22.6	37.1	43.8
7.50	388.8	100.7	42.7	25.1	40.2	43.9
7.70	382.1	100.3	43.3	30.2	41.5	46.9
7.90	381.3	96.9	43.5	31.5	46.8	51.2
8.10	380.4	93.1	45.2	35.3	51.9	57.5
8.31	383.1	90.0	47.4	40.3	57.0	64.8
8.51	385.0	83.8	52.1	45.1	63.6	75.3
8.71	405.2	75.5	58.2	51.2	81.5	94.7
8.91	408.9	64.7	62.3	57.8	90.3	111.5
9.11	429.8	53.2	69.1	63.8	101.4	136.0
9.31	451.8	38.3	74.7	66.6	109.2	166.1
9.51	469.8	25.7	78.8	67.3	122.8	189.0
9.72	486.2	15.6	82.7	64.8	127.1	208.4
9.92	493.8	9.9	81.1	57.3	125.7	220.0
10.12	488.9	10.0	77.0	49.4	121.4	218.7
10.32	474.8	13.4	73.2	40.3	109.8	207.5
10.52	458.1	18.2	67.9	32.3	99.3	196.8
10.72	437.0	24.6	62.8	25.4	90.6	183.0
10.92	420.2	30.9	55.9	19.7	81.9	165.6

The alpha energy is given in the lab system. The scattering angle and cross section are in the centre-of-mass system.

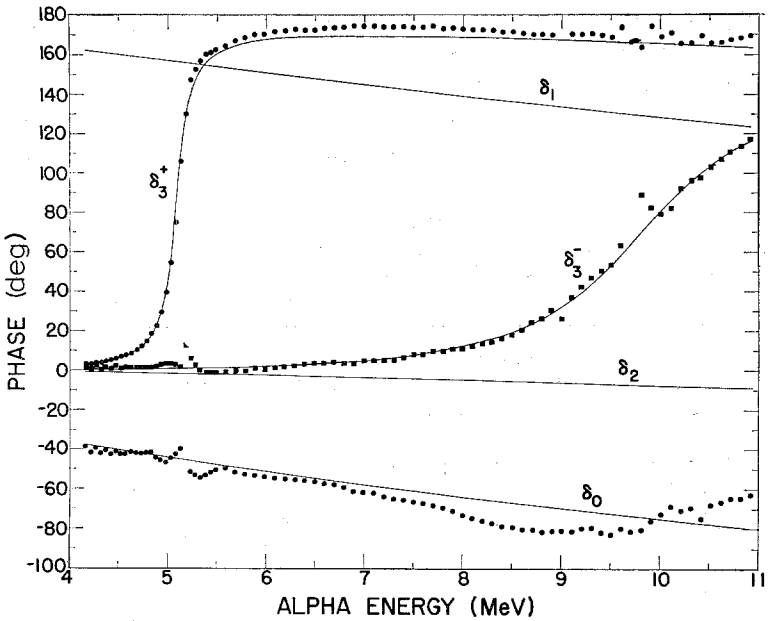

Fig. 10. The phase shifts obtained from the excitation functions of fig. 9. The curves associated with δ_0, δ_1 and δ_2 represent charged hard-sphere values as described in the text. The curves associated with δ_3^+ and δ_3^- were computed from the resonance parameters of table 10.

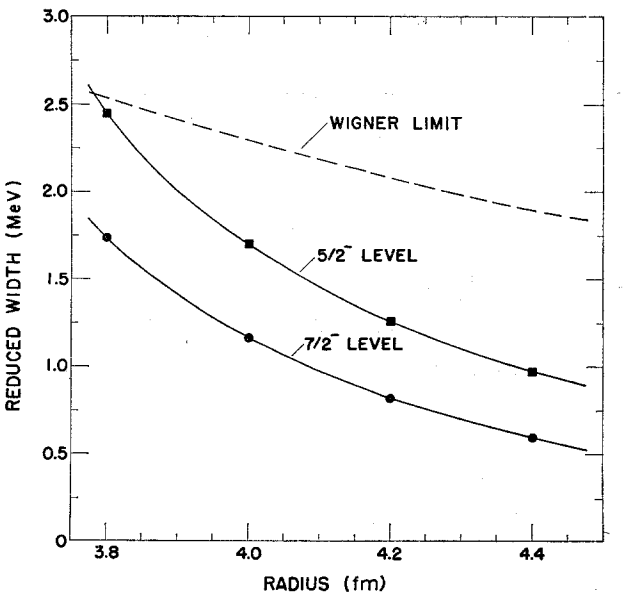

Fig. 11. A plot of reduced width versus radius for which satisfactory fits were obtained to the $l = 3$ phase shifts of fig. 10.

Single level parameterizations of δ_3^+ and δ_3^- were attempted using the formulae of Lane and Thomas [18]). Values of the reduced width γ^2 were obtained which gave the best fit to the phase shifts of fig. 10 for various values of R. In obtaining the fits, the energies at which the total phase shifts went through 90° were constrained to be 5.084 MeV and 10.20 MeV lab alpha energy. These energies were obtained from the δ_3^+

TABLE 10

Resonance parameters for the $^2F_{\frac{7}{2}}$ and $^2F_{\frac{5}{2}}$ levels in ^{7}Li obtained from the phase shifts of fig. 10

Configuration	$J\pi$	E_{res}(MeV)	E_x(MeV)	R(fm)	γ^2(MeV)	θ^2
$^2F_{\frac{7}{2}}$	$\frac{7}{2}^-$	5.08±0.01	4.65±0.02	4.4	0.60	0.32
$^2F_{\frac{5}{2}}$	$\frac{5}{2}^-$	10.07±0.20	6.79±0.09	4.4	0.98	0.52

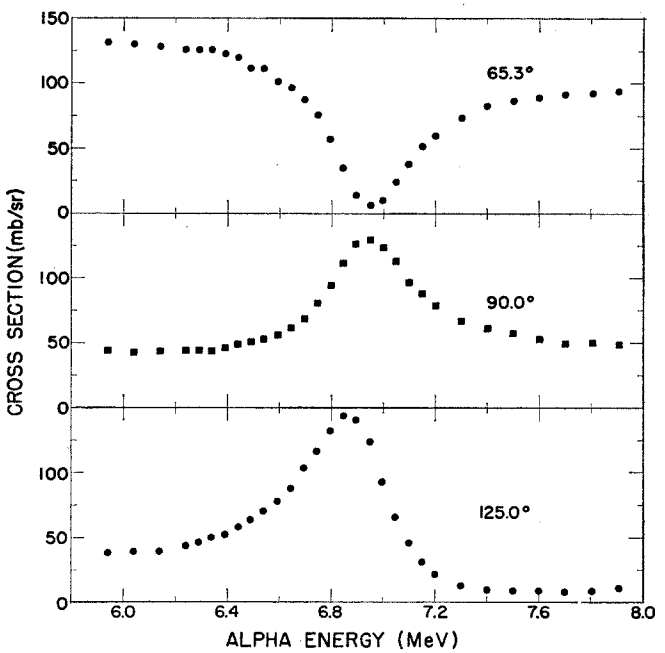

Fig. 12. Excitation functions for ^{4}He-^{3}He elastic scattering. The scattering angle and differential cross section are given in the centre-of-mass system. The energy scale is in the lab system.

and δ_3^- points in fig. 10. Values of R = 3.8 fm to 4.4 fm were found to give fits of approximately equal quality. A summary of the values of γ^2 and R which fit the F-wave phase shifts is given in fig. 11.

The resonance parameters obtained for a radius of 4.4 fm are listed in table 10. The quantity E_{res} is the lab alpha energy at which the resonant part of the phase shift goes through 90°. The quantity E_x is the corresponding excitation energy. The ratio

of the extracted width to the Wigner limit is given by θ^2. In fig. 10 the solid curves associated with δ_3^+ and δ_3^- represent the fits obtained with these parameters. The uncertainty of 200 keV in E_{res} for the $\frac{5}{2}^-$ level results from sensitivity to the manner in which the P- and D-wave phase shifts were constrained. The quoted error in E_{res} for the $\frac{7}{2}^-$ level results almost entirely from uncertainty in the thickness of the gas target entrance foil.

As stated earlier, three excitation functions for ^{4}He-^{3}He elastic scattering were measured using the same gas target and entrance foil as were used for the ^{4}He-^{3}H measurements in order to accurately measure the difference in energy of the $^2F_{\frac{7}{2}}$ level

TABLE 11

^{4}He-^{3}He elastic scattering excitation function data

E_α (MeV)	σ(65.3°) (mb/sr)	σ(90.0°) (mb/sr)	σ(125.0°) (mb/sr)	E_α (MeV)	σ(65.3°) (mb/sr)	σ(90.0°) (mb/sr)	σ(125.0°) (mb/sr)
5.94	130.8	44.6	37.6	6.846	35.1	110.8	143.6
6.04	130.6	42.6	38.6	6.896	13.8	126.2	141.1
6.14	128.4	43.0	38.9	6.947	5.7	129.0	123.7
6.24	126.3	43.5	43.9	6.997	9.8	123.4	92.7
6.29	125.8	44.1	45.6	7.048	23.4	116.2	66.5
6.34	125.8	43.4	49.9	7.098	37.4	97.0	45.9
6.39	123.3	46.6	52.4	7.149	50.9	87.7	30.9
6.44	120.6	49.2	58.4	7.199	59.7	79.1	22.1
6.49	112.1	51.1	63.6	7.300	73.8	66.7	13.0
6.54	111.9	52.5	69.6	7.401	83.3	61.5	9.6
6.594	102.4	55.8	77.7	7.50	86.8	57.6	8.9
6.644	97.2	60.9	87.8	7.60	88.7	53.0	8.8
6.694	88.6	67.4	103.5	7.70	91.8	49.7	8.0
6.745	75.6	79.7	115.6	7.80	92.8	49.8	9.3
6.796	57.1	94.3	132.4	7.90	93.8	48.5	11.0

The alpha energy is given in the lab system. The scattering angle and cross section are in the centre-of-mass system.

in ^{7}Li and ^{7}Be. The ^{4}He-^{3}He excitation functions are presented in fig. 12 and in table 11. Statistical errors in these data are 3 % or less. The energy range was chosen to span the $\frac{7}{2}^-$ level in ^{7}Be.

In order to obtain the energy difference accurately, it was felt desirable to obtain the resonance energy from these data by a fitting technique. However, since only three excitation functions were available, a phase-shift analysis of the ^{4}He-^{3}He data was not feasible. Instead, it was decided to fit the ^{4}He-^{3}He and refit the ^{4}He-^{3}H cross-section data directly in terms of $^2F_{\frac{7}{2}}$ resonance parameters. With the exception of δ_3^- and δ_3^+, the phase shifts were constrained to appropriate hard-sphere values. The phase shift δ_3^- was computed from the resonance parameters given in table 10 in the case of ^{7}Li and from the parameters of Tombrello and Parker [16]) in the case

of ^{7}Be. The remaining phase shift (δ_3^+) was computed from various values of E_{res} and γ^2 until best fits were obtained to the data.

The results of this analysis are given in table 12. The difference in excitation energy of the $^2F_{\frac{7}{2}}$ level in ^{7}Li and ^{7}Be is seen to be 88 keV. The error in this value is estimated to be ± 7 keV largely resulting from sensitivity to the particular choice of the non-resonant phase shifts.

TABLE 12

Resonance parameters for the $^2F_{\frac{7}{2}}$ levels in ^{7}Li and ^{7}Be

	Present work		Published values [19])
	^{7}Li	^{7}Be	^{7}Be
E_x(MeV)	4.654	4.566	4.54
R(fm)	4.4	4.4	4.4
θ^2	0.37	0.34	0.36

These parameters were obtained by fitting the excitation functions directly as described in the text.

The authors would like to express thanks to Mr. G. P. Clarkson for his help with the drawings used in this paper. The authors are indebted to Professor E. W. Titterton for his interest and support during the experiment.

References

1) G. G. Ohlsen and P. G. Young, Nucl. Phys. **52** (1964) 134
2) C. H. Johnson and H. E. Banta, Rev. Sci. Instr. **27** (1956) 132
3) Nelson Jarmie, M. G. Silbert, D. M. Smith and J. S. Loos, Phys. Rev. **130** (1963) 1987
4) H. W. Lefevre, R. R. Borchers and C. H. Poppe, Phys. Rev. **128** (1962) 1328;
P. G. Young and G. G. Ohlsen, Phys. Lett. **8** (1964) 124;
N. Jarmie, R. H. Stokes, G. G. Ohlsen and R. W. Newsome, Jr., Phys. Rev. **161** (1967) 1050
5) B. R. Barrett, J. D. Walecka and W. E. Meyerhof, Phys. Lett. **22** (1966) 450
6) N. A. Vlasov and L. N. Samoilov, Atom. Energ. **17** (1964) 3 [translation: UCRL-1183, Feb.1965]
7) T. A. Tombrello, Phys. Rev. **138** (1965) B40
8) J. E. Brolley, Jr., T. M. Putnam, L. Rosen and L. Stewart, Phys. Rev. **117** (1960) 1307
9) T. Lauritsen and F. Ajzenberg-Selove, Nucl. Phys. **78** (1966) 1
10) S. J. Bame, Jr., and J. E. Perry, Jr., Phys. Rev. **107** (1957) 1616
11) T. A. Tombrello, R. J. Spiger and A. D. Bacher, Phys. Rev. **154** (1967) 935
12) J. Cerny, C. Détraz and R. H. Pehl, Phys. Rev. **152** (1966) 950
13) W. R. Stratton, G. D. Freier, G. R. Keepin, D. Rankin and T. F. Stratton, Phys. Rev. **88** (1952) 257
14) W. T. Leland, J. E. Brolley, Jr. and L. Rosen, Bull. Am. Phys. Soc. **10** (1965) 51
15) D. R. Thompson and Y. C. Tang, Bull. Am. Phys. Soc. **12** (1967) 893
16) T. A. Tombrello and P. D. Parker, Phys. Rev. **130** (1963) 1112
17) C. L. Critchfield and D. C. Dodder, Phys. Rev. **76** (1949) 602
18) A. M. Lane and R. G. Thomas, Revs. Mod. Phys. **30** (1958) 257
19) P. D. Miller and G. C. Phillips, Phys. Rev. **112** (1958) 2048